Study of Chemically Reactive Flow and Heat Transfer in the Presence of a Uniform Magnetic Field

Mehrabian, Mozaffar Ali*[+]; Kimiaeifar, Ali; Golkarfard, Vahid; Akhgar, Ali Reza
Department of Mechanical Engineering, Shahid Bahonar University of Kerman, Kerman, I.R. IRAN

ABSTRACT: *The effects of chemical reaction, thermal stratification, Soret and Dufour numbers on magneto-hydrodynamic free convective heat and mass transfer of a viscous, incompressible, and electrically conducting fluid on a vertical stretching surface embedded in a saturated porous medium are presented. A similarity transform is used to reduce the governing partial differential equations into a system of nonlinear ordinary differential equations, which is solved analytically by means of homotopy analysis method. The results are compared with numerical predictions obtained by fourth order Runge-Kutta method. Close agreement is observed between the two sets of results. The method is led to an expression, which is acceptable for all values of effective parameters and controls the convergence of the solution.*

KEYWORDS: *Magneto-HydroDynamic (MHD) Flow; Similarity solution; Homotopy Analysis Method (HAM); Soret Number; Dufour number*.

INTRODUCTION

The effects of chemical reaction, thermal stratification, Soret and Dufour numbers on MHD free convective heat and mass transfer of viscous, incompressible and electrically conducting fluid on a vertical stretching surface embedded in a saturated porous medium are investigated analytically. The flow field in porous media is influenced appreciably by the presence of chemical reaction, thermal stratification, Soret number, Dufour number, and magnetic field. *Kandasamy et al.* [1] have discussed the internal heat generation and thermal stratification effects on MHD flow over an accelerating vertical surface. *Alam et al.* [2] have discussed the local similarity solutions for unsteady MHD free convection heat and mass transfer flow past an impulsively started vertical porous plate with Soret and Dufour effects. *Alam et al.* [3] have investigated the effects of Dufour and Soret numbers on unsteady MHD free convection heat and mass transfer past a vertical porous plate embedded in a porous medium. *Raptis et al.* [4] have studied the MHD free convection heat and mass transfer through porous medium bounded by an infinite vertical porous plate with constant heat flux. *Anghel et al.* [5] have investigated the Dufour and Soret effects on free convection boundary layer over a vertical surface embedded in a porous medium. *Postelnicu* [6] studied the influence of a magnetic field on heat and mass transfer by natural convection from vertical surfaces embedded in porous media taking into account the Soret and Dufour effects. *Alam et al.* [7] presented the Dufour and Soret effects on MHD free convective heat and mass transfer flow past a vertical flat plate embedded in a porous medium. The chemical reaction, heat and mass transfer

* *To whom correspondence should be addressed.*
+ E-mail: ma_mehrabian@alum.mit.edu
1021-9986/2016/3/119-137 *19/$/6.90*

on MHD flow over a vertical isothermal conic surface in micro-polar fluids have been investigated by *El-Kabeir et al.* [8]. *Mansour et al.* [9] discussed the effects of chemical reaction and thermal stratification on MHD free convective heat and mass transfer over a vertical stretching surface embedded in a porous medium considering Soret and Dufour numbers.

Homotopy Analysis Method (HAM), first proposed by *Liao* [10], is one of the semi-exact methods that has been used to solve many problems in solid and fluid mechanics [11-20]. In this method the convergence region can be adjusted and controlled, which is the most important feature of this technique in comparison with numerical and perturbation methods. Numerical methods involve the satisfaction of stability and convergence criteria, otherwise non-physical or inappropriate results appear, on the other hand the solution domain should cover all values of the effective parameters. Perturbation methods, however, require the solution of the governing equation while a small parameter is inserted in the equation. The Homotopy Analysis Method (HAM), is neither restricted by stability and convergence considerations (as the numerical methods are), nor by finding a small parameter and inserting into the governing equation (as the perturbation methods are).

Up to now, no investigation has been made which provides the analytical solution for MHD free convective heat and mass transfer of viscous, incompressible and electrically conducting fluid on a vertical stretching surface embedded in a saturated porous medium considering Soret and Dufour numbers. In this study, HAM is applied to find an analytical solution for nonlinear ordinary differential equations arising from the similarity solution, and the results are compared with the numerical solution based on shooting method and fourth order Runge-Kutta method.

THEORITICAL SECTION

Mathematical formulation

Two-dimensional steady nonlinear MHD free convective heat and mass transfer of incompressible, viscous, and electrically conducting flow in the presence of a uniform magnetic field is studied. Thermal stratification, chemical reaction, and Soret and Dufour effects in porous medium boundary layer have been taken into account. This system is shown in Fig.1. According to the coordinate system, the *x*-axis is chosen parallel to the vertical surface and the *y*-axis is taken normal to it. A transverse magnetic field of strength B_0 is applied parallel to the *y*-axis. The governing equations for this case are as follows [9]:

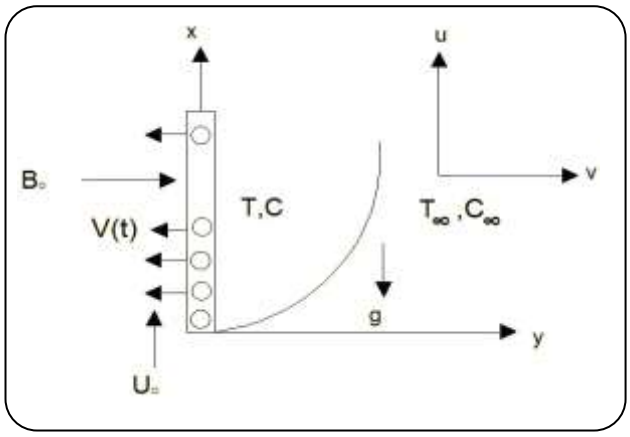

Fig. 1: Schematic diagram of a vertical stretching surface in a porous medium.

$$f''' + Gr_x\,Re_x\,\theta + Gc_x\,Re_x\,\varphi - \left(M^2\,Re_x + Re_x/K\right)f' - f'^2 + ff'' = 0 \quad (1)$$

$$\theta'' + Pr\left(Du\phi'' - nf'\theta + f\theta'\right) = 0 \quad (2)$$

$$\phi'' + Sc\left(Sr\theta'' - \gamma\,Re_x\,\phi - n_1 f'\phi + f\phi'\right) = 0 \quad (3)$$

In the above equations, primes show differentiation with respect *to* η, $f(\eta)$ is the dimensionless stream function, $\theta(\eta)$ is the dimensionless temperature of the fluid in the boundary layer, $\phi(\eta)$ is the dimensionless concentration of the fluid in the boundary layer. ($Re_x=U_0X/\nu$) is the Reynolds number, $Gr_x = \nu g\beta_T\left(T_w - T\infty\right)/U_0^3$ is the Grashof number [9], $Gc_x = \nu g\beta_c\left(C_w - C\infty\right)/U_0^3$ is the modified Grashof number [9], $Pr = \mu C_p/k$ is the Prandtl number, $Sc=\nu/D_m$ is the Schmidt number, $M^2 = \sigma B_0^2\nu/\rho U_0^2$ is the magnetic parameter, $K = K_1U^2/\nu^2$ is the permeability parameter, $\gamma = \nu K_c/U_0^2$ is the chemical reaction parameter, $Du = \left(D_mK_T/\nu C_s\,C_p\right)\left(C_w - C_\infty/T_w\,T_\infty\right)$ is the Dufour number, and $Sr = \left(D_mK_T/\nu T_m\right)\left(T_w - T_\infty/C_w - C_\infty\right)$ is the Soret number. The physical properties ρ, μ, D and K_c (rate of chemical reaction) are constant throughout

the fluid. *n*. is the thermal stratification parameter which is a constant and has a quantity between zero and one $0 \le n \le 1$.

B_0, σ and T are the strength of magnetic field, the electrical conductivity of the fluid, and the temperature, respectively. β_T is the isothermal coefficient of volume expansion, and β_C the volumetric coefficient of expansion with concentration. ν, K_1 and D_m are kinematic viscosity, permeability of porous medium, and coefficient of mass diffusivity, respectively. C_p is the specific heat at constant pressure, T_m the mean fluid temperature, K_T the thermal diffusion ratio, and C_s the concentration susceptibility. The boundary conditions for Eqs. (1-3) are:

$$f(0) = 0 f'(0) = 1 \theta(0) = 1 \phi(0) = 1 \tag{4}$$

$$\theta(\infty) = 0 \phi(\infty) = 0 \tag{5}$$

Application of HAM

The governing equations for MHD free convective heat and mass transfer over a vertical stretching surface embedded in a porous medium are expressed by Eqs. (1-3). Nonlinear operators are defined as follows:

$$N_f\left[f(\eta;q)\right] = \frac{\partial^3(\eta;q)}{\partial\eta^3} + Gr_x\, Re_x\, \theta(\eta;q) + \tag{6}$$

$$Gc_x\, Re_x\, \varphi(\eta;q) - \left(M^2\, Re_x + \frac{Re_x}{K}\right)\frac{\partial f(\eta;q)}{\partial\eta} -$$

$$\left(\frac{\partial f(\eta;q)}{\partial\eta}\right)^2 + f(\eta;q)\frac{\partial^2 f(\eta;q)}{\partial\eta^2}$$

$$N_\theta\left[\theta(\eta;q)\right] = \frac{\partial^2\theta(\eta;q)}{\partial\eta^2} + Pr\left(Du\frac{\partial^2\varphi(\eta;q)}{\partial\eta^2} - \right. \tag{7}$$

$$\left. n\frac{\partial f(\eta;q)}{\partial\eta}\theta(\eta;q) + f(\eta;q)\frac{\partial\theta(\eta;q)}{\partial\eta}\right)$$

$$N_\varphi\left[\varphi(\eta;q)\right] == \frac{\partial^2\varphi(\eta;q)}{\partial\eta^2} + Sc\left(Sr\frac{\partial^2\theta(\eta;q)}{\partial\eta^2} - \right. \tag{8}$$

$$\left. \gamma\, Re_x\, \varphi(\eta;q) - n_1\frac{\partial f(\eta;q)}{\partial\eta}\varphi(\eta;q) + f(\eta;q)\frac{\partial\varphi(\eta;q)}{\partial\eta}\right)$$

where, $q \in [0, 1]$ is the embedding parameter. As the embedding parameter is increased from *0* to *1*, $U(\eta; q)$, $Y(\eta;q)$ and $V(\eta;q)$ vary from the initial guess, $U_0(\eta)$, $Y_0(\eta)$ and $V_0(\eta)$, to the exact solution, $U(\eta)$, $Y(\eta)$ and $V(\eta)$.

$$f(\eta;0) = U_0(\eta) \ , \ f(\eta;1) = U(\eta) \tag{9}$$

$$\theta(\eta;0) = Y_0(\eta) \quad , \quad \theta(\eta,1) = Y(\eta) \tag{10}$$

$$\phi(\eta;0) = V_0(\eta) \quad , \quad \phi(\eta;1) = V(\eta) \tag{11}$$

Expanding $f(\eta;q)$, $\theta(\eta;q)$ and $\phi(\eta;q)$ in Taylor series with respect to q results in:

$$f(\eta;q) = U_0(\eta) + \sum_{m=1}^{\infty} U_m(\eta) q^m \tag{12}$$

$$\theta(\eta;q) = Y_0(\eta) + \sum_{m=1}^{\infty} Y_m(\eta) q^m \tag{13}$$

$$\phi(\eta;q) = V_0(\eta) + \sum_{m=1}^{\infty} V_m(\eta) q^m \tag{14}$$

where,

$$U_m(\eta) = \frac{1}{m!}\frac{\partial^m f(\eta;q)}{\partial q^m}\bigg|_{q=0} \tag{15}$$

$$Y_m(\eta) = \frac{1}{m!}\frac{\partial^m \theta(\eta;q)}{\partial q^m}\bigg|_{q=0} \tag{16}$$

$$V_m(\eta) = \frac{1}{m!}\frac{\partial^m \phi(\eta;q)}{\partial q^m}\bigg|_{q=0} \tag{17}$$

Homotopy Analysis Method (HAM) can be expressed by many different base functions [10], according to the governing equations; it is straightforward to use a base function in the form of:

$$U(\eta) = \sum_{m=1}^{\infty}\sum_{p=1}^{\infty} b_{pm}\eta^p e^{-m\eta} \tag{18}$$

$$Y(\eta) = \sum_{m=1}^{\infty}\sum_{p=1}^{\infty} d_{pm}\eta^p e^{-m\eta} \tag{19}$$

$$V(\eta) = \sum_{m=1}^{\infty}\sum_{p=1}^{\infty} k_{pm}\eta^p e^{-m\eta} \tag{20}$$

b_{pm}, d_{pm}, and k_{pm} are the coefficients to be determined. When the base function is selected, the auxiliary

functions $H_f(\eta)$ and $H_g(\eta)$, initial approximations $U_0(\eta)$ and $Y_0(\eta)$ and the auxiliary linear operators L_f and L_g must be chosen in such a way that the corresponding high-order deformation equations have solutions with the functional form similar to the base function. It is worth mentioning that the presence of expressions such as $\eta sin(m\eta)$ prevents the convergence of the analytical solution. This method is referred to as the rule of solution expression [10]. The linear operators L_f , L_θ and L_ϕ are chosen as:

$$L_f\left[f(\eta;q)\right]=\frac{\partial^3 f(\eta;q)}{\partial\eta^3}-\frac{\partial f(\eta;q)}{\partial\eta} \quad (21)$$

$$L_\theta\left[\theta(\eta;q)\right]=\frac{\partial^2\theta(\eta;q)}{\partial\eta^2}-\frac{\partial\theta(\eta;q)}{\partial\eta} \quad (22)$$

$$L_\varphi\left[\varphi(\eta;q)\right]=\frac{\partial^2\varphi(\eta;q)}{\partial\eta^2}-\frac{\partial\varphi(\eta;q)}{\partial\eta} \quad (23)$$

Eq. 16 and Eq. 17 result in:

$$L_f\left[c_1+c_2e^{\eta}+c_3e^{-\eta}\right]=0 \quad (24)$$

$$L_\theta\left[c_4+c_5e^{-\eta}\right]=0 \quad (25)$$

$$L_\phi\left[c_6+c_7e^{-\eta}\right]=0 \quad (24)$$

Where c_1 to c_7 are the integral constants. According to the rule of solution expression and the initial conditions, the initial approximations, U_0 and Y_0 as well as the integral constants, c_1 to c_6 are expressed as:

$$U_0(\eta)=c_1+c_2e^{\eta}+c_3e^{-\eta} \quad (27)$$
$$c_1=1\ ,\ c_2=0\ ,\ c_3=-1$$

$$Y_0(\eta)=c_4+c_5e^{-\eta} \quad (28)$$
$$c_4=0\ ,\ c_5=1$$

$$V_0(\eta)=c_6+c_7e^{-\eta} \quad (29)$$
$$c_6=0\ ,\ c_7=1$$

The 0th order deformation equations and their boundary conditions are:

$$(1-q)L_f\left[f(\eta;q)-U_0(\eta)\right]= \quad (30)$$
$$q\hbar_f H_f(\eta)N_f\left[f(\eta;q)\right]$$

$$f(0;q)=0\ ,\ \frac{\partial f(0;q)}{\partial\eta}=1\ ,\ \frac{\partial f(\infty;q)}{\partial\eta}=0 \quad (31)$$

$$(1-q)L_\theta\left[\theta(\eta;q)-Y_0(\eta)\right]= \quad (32)$$
$$q\hbar_\theta H_\theta(\eta)N_\theta\left[\theta(\eta;q)\right]$$

$$\theta(0;q)=1\ ,\ \frac{\partial\theta(\infty;q)}{\partial\eta}=0 \quad (33)$$

$$(1-q)L_\phi\left[\phi(\eta;q)-V_0(\eta)\right]= \quad (34)$$
$$q\hbar_\phi H_\phi(\eta)N_\phi\left[\phi(\eta;q)\right]$$

$$\phi(0;q)=1\ ,\ \frac{\partial\phi(\infty;q)}{\partial\eta}=0 \quad (35)$$

According to the rule of solution expression and from Eq. (15), the auxiliary function $H(\eta)$ can be chosen as follows:

$$H_f(\eta)=\eta^p e^{-m\eta} \quad (36)$$

$$H_\theta(\eta)=\eta^p e^{-m\eta} \quad (37)$$

$$H_\phi(\eta)=\eta^p e^{-m\eta} \quad (38)$$

Differentiating Eqs. (21-23), m times, with respect to the embedding parameter q, then setting $q=0$ in the final expression, and dividing by $m!$, these equations are reduced to the mth order deformation equation:

$$U_m(\eta)=\chi_m U_{m-1}(\eta)+\gg\frac{1}{2}\int_0^{\eta}H_f(\eta)R_m(U_{m-1})d\eta- \quad (39)$$
$$\frac{1}{2}e^{-q}\int_0^{\eta}H_f(\eta)e^{\eta}R_m(U_{m-1})d\eta+c_1+c_2e^{\eta}+c_3e^{-\eta}$$

$$U_m(0)=0\ \ ,\ \ U'_m(0)=0\ \ ,\ \ U'_m(\infty)=0 \quad (40)$$

$$Y_m(\eta)=\chi_m Y_{m-1}(\eta)+ \quad (41)$$
$$\hbar\int_0^{\eta}\int_0^{\mu}H_\theta(\eta)e^{\eta}R_m(Y_{m-1})d\eta d\mu+c_4+c_5e^{-\eta}$$

$$U_m(0)=0\ \ ,\ \ U'_m(\infty)=0 \quad (42)$$

$$V_m(\eta)=\chi_m V_{m-1}(\eta)+ \quad (43)$$
$$\hbar\int_0^{\eta}\int_0^{\mu}H_\phi(\eta)e^{\eta}R_m(V_{m-1})d\eta d\mu+c_4+c_5e^{-\eta}$$

$$V_m(0)=0\ \ ,\ \ V'_m(\infty)=0 \quad (44)$$

Where

$$R_m(U_{m-1}) = \frac{d^3U_{m-1}(\eta)}{d\eta^3} + Gr_x\, Re_x\, Y(\eta) + \quad (45)$$

$$Gc_x\, Re_x\, V(\eta) - (M^2\, Re_x + \frac{Re_x}{K})\frac{dU_{m-1}(\eta)}{d\eta} -$$

$$\sum_{z=0}^{m-1}\frac{dU_z(\eta)}{d\eta}\frac{dU_{m-1-z}(\eta)}{d\eta} + \sum_{z=0}^{m-1}U_z(\eta)\frac{d^2U_{m-1-z}(\eta)}{d\eta^2}$$

$$R_m(V_{m-1}) = \frac{d^2V_{m-1}(\eta)}{d\eta^2} + Sc\left(Sr\frac{d^2Y_{m-1}(\eta)}{d\eta^2} - \right. \quad (46)$$

$$\gamma\, Re_x\, V_{m-1}(\eta) - n_1\sum_{z=0}^{m-1}V_z(\eta)\frac{dU_{m-1-z}(\eta)}{d\eta} +$$

$$\left.\sum_{z=0}^{m-1}U_z(\eta)\frac{dV_{m-1-z}(\eta)}{d\eta}\right)$$

$$R_m(V_{m-1}) = \frac{d^2V_{m-1}(\eta)}{d\eta^2} + Sc\left(Sr\frac{d^2Y_{m-1}(\eta)}{d\eta^2} - \right. \quad (47)$$

$$\gamma\, Re_x\, V_{m-1}(\eta) - n_1\sum_{z=0}^{m-1}V_z(\eta)\frac{dU_{m-1-z}(\eta)}{d\eta} +$$

$$\left.\sum_{z=0}^{m-1}U_z(\eta)\frac{dV_{m-1-z}(\eta)}{d\eta}\right)$$

$$\chi_m = \begin{cases} 0, & m \le 1 \\ 1, & m > 1 \end{cases} \quad (48)$$

The rate of convergence can be increased when suitable values are selected for *m* and *p*. According to *the* rule of solution expression the suitable values for *m* and *p* are {*p=0, m=1*}. Consequently, the corresponding auxiliary function was determined as $H_f(\eta) = e^{-\eta}$. As a result of this selection, the first and second terms of the solution's series are as follows:

$$U_0(\eta) = 1 - e^{-\eta} \quad (49)$$

$$U_1(\eta) = \frac{0.5h\, Re_x}{K}\left(1 + M^2K - Gr_xK - Gc_xK - \right. \quad (50)$$

$$e^{-\eta} + Gc_xKe^{-\eta} + Gr_xKe^{-\eta} + \eta Gr_xKe^{-\eta} -$$

$$\left.M^2Ke^{-\eta} + \eta\gamma Ke^{-\eta} - \eta M^2Ke^{-\eta} - \eta e^{-\eta}\right)$$

$$Y_0(\eta) = e^{-\eta} \quad (51)$$

$$Y_1(\eta) = h\,Pr\,Du - 0.3333h\,Pr - 0.6666h\,Pr\,n - \quad (52)$$

$$1.5h\,Pr\,Du\,e^{-\eta} + 0.8333h\,Pr\,ne^{-\eta} + 0.6667h\,Pr\,e^{-\eta} +$$

$$0.5he^{-2\eta} + 0.5h\,Pr\,Due^{-2\eta} - 0.1667h\,Pr\,ne^{-3\eta} -$$

$$0.5h\,Pr\,e^{-2\eta} + 0.1667h\,Pr\,e^{-3\eta} + h - 1.5he^{-\eta}$$

$$V_0(\eta) = e^{-\eta} \quad (53)$$

$$V_1(\eta) = 0.5hSc\gamma\, Re_x\, e^{-\eta} - 0.5hScSre^{-\eta} + \quad (54)$$

$$0.1667hScne^{-\eta} + 0.3333hSce^{-\eta} + 0.5he^{-2\eta} -$$

$$0.5hSc\, Re_x\, \gamma e^{-2\eta} + 0.5hScSre^{-2\eta} - 0.1667hScne^{-3\eta} -$$

$$0.5hSce^{-2\eta}\, 0.1667hSce^{-3\eta} - 0.5he^{-\eta}$$

Convergence of HAM Solution

The analytical solution should converge. It should be noted that the auxiliary parameter $\hbar$, as pointed out by *Liao* [10], controls the convergence and accuracy of the solution series. In order to define a region such that the solution series is independent of $\hbar$, a multiple of $\hbar$-curves are plotted. The region where the distributions of *f*'', *f*', *f*, θ, θ' and ϕ, ϕ' versus $\hbar$ are horizontal lines, is known as the convergence region for the corresponding function. The common region among the $f(\eta)$ and its derivatives, $\theta(\eta)$ and its derivative, and $\phi(\eta)$ and its derivative is known as the overall convergence region.

To study the effect of $\hbar$ on the convergence of solution, the $\hbar$-curves of *f*''(0.5), *f*'(2), *f*(1), θ'(0), θ(1), ϕ'(0) and ϕ(1) are plotted by 12th order approximation of solution for selected values of constant numbers, as shown in Fig. 2.

RESULTS AND DISCUSSION

HAM has been applied for different values of M^2, Du, Sr, γ, n, Sc, Pr and for fixed values of Gr_x=1, Gc_x=2, Re_x=1, K=1 and n_1=0.5 to obtain a clear insight of the physical problem, the results are listed in the tables and illustrated in the figures. HAM results summarized in Tables 1–12, have been compared with the results obtained by numerical methods, as well as with the results obtained in [9]. The velocity profiles for different values of Soret and Dufour numbers are presented in Fig. 3. It is seen that the velocity of fluid is decreased as the Soret number is decreased or the Dufour number is increased. Fig. 4 represents the temperature profiles for different values of Soret and Dufour numbers and

Table 1: Comparison of analytical, numerical, and [9] results of $f''(0)$, $\theta'(0)$ and $\phi'(0)$ for various values of Sr and Du, with M^2=1, Re_x=1, γ= 1, Pr= 0.71, Sc= 0.62, n= 0.5, Cr_x=1, Gc_x= 2 and K=1.

$f''(0)$					$\theta'(0)$			$\phi'(0)$		
Du	Sr	HAM	Num	Ref[9]	HAM	Num	Ref[9]	HAM	Num	Ref [9]
0.03	2	-0.5121	-0.5113	-0.5399	-0.7263	-0.7263	-0.7731	-0.6743	-0.6725	-0.6707
0.12	1	-0.5690	-0.5691	-0.5986	-0.6674	-0.6674	-0.8210	-0.8831	-0.8590	-0.8350
0.3	0.5	-0.5867	-0.5868	-0.6399	-0.5671	-0.5672	-0.9395	-0.9879	-0.9813	-0.9113
0.6	0.1	-0.5885	-0.5885	-0.6980	-0.4030	-0.4030	-1.1612	-1.0463	-1.0258	-1.0052

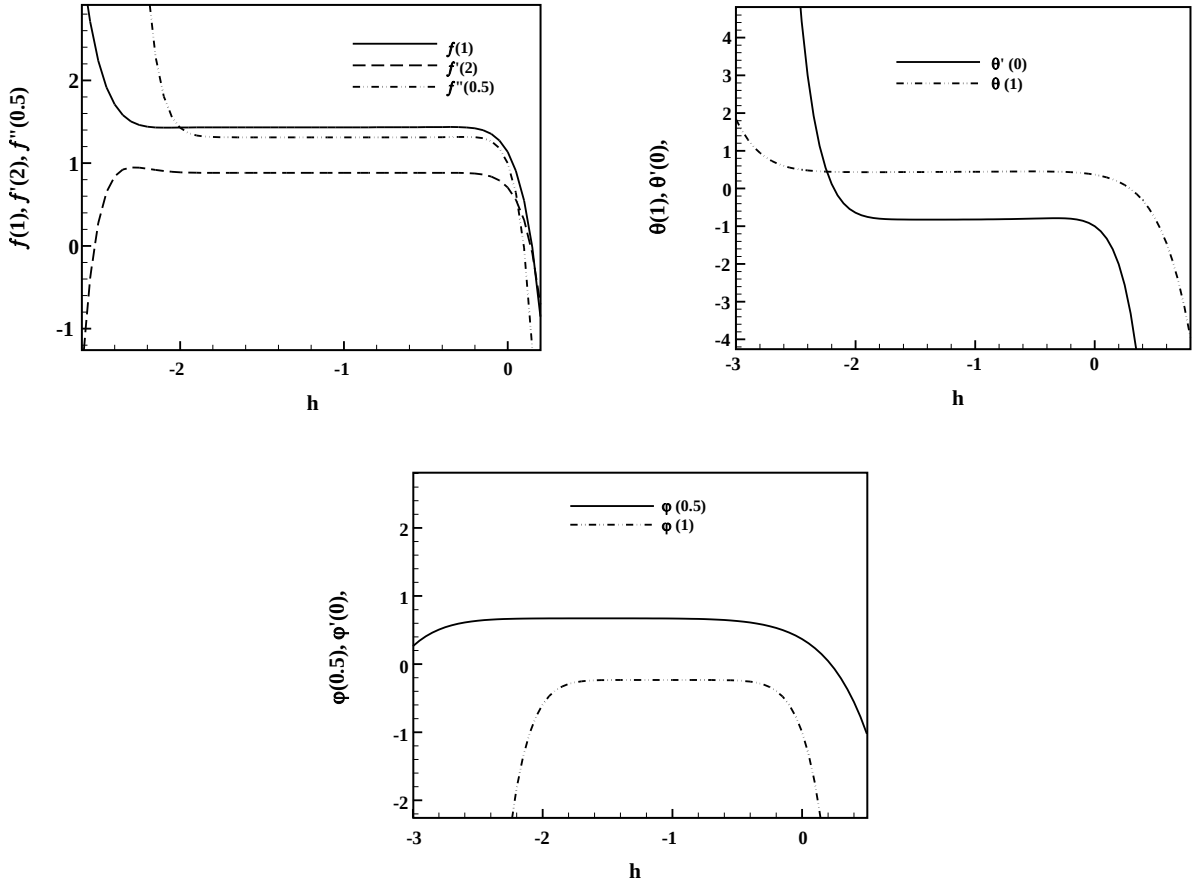

Fig. 2: The ħ curves to indicate the convergence region of MHD free convective heat and mass transfer over a vertical stretching surface in a porous medium, M^2=1, Re=1, γ= 1, Pr= 0.71, Sc= 0.62, η = 0.5, Gr=1, Gc= 2 and K=1.

constant chemical reaction and thermal stratifications parameters. It is understood that the temperature of fluid is increased when the Soret number is decreased or the Dufour number is increased. Fig. 5 represents the concentration profiles for different Soret and Dufour numbers but constant chemical reaction and thermal stratification parameters. It is observed that the concentration of fluid is decreased when decreasing the Soret number or increasing the Dufour number. Figs. 6–8 show the effect of chemical reaction on velocity, temperature and concentration respectively. It is understood that when increasing the chemical reaction parameter, the velocity and concentration are decreased and a small change is occurred in temperature profiles.

Table 2: Comparison of analytical, numerical, and [9] results of $f''(\infty)$, $\theta'(\infty)$ and $\phi'(\infty)$ for various values of Sr and Du, with M^2=1, Re_x=1, γ= 1, Pr= 0.71, Sc= 0.62, n= 0.5, Gr_x=1, Gc_x= 2 and K=1.

$f''(\infty)$					$\theta'(\infty)$			$\phi'(\infty)$		
Du	Sr	HAM	Num	Ref[9]	HAM	Num	Ref[9]	HAM	Num	Ref[9]
0.03	2	-0.0009	-0.0009	-0.1164	-0.0004	-0.0004	-0.0795	-0.0015	-0.0014	-0.1700
012	1	-0.0009	-0.0009	-0.0980	-0.0009	-0.0008	-0.0726	-0.0012	-0.0011	-0.1149
03	05	-0.0009	-0.0009	-0.0847	-0.0013	-0.0013	-0.0495	-0.0008	-0.0008	-0.0877
06	01	-0.0007	-0.0007	-0.0680	-0.0017	-0.0016	-0.0093	-0.0002	-0.0002	-0.0657

Table 3: Comparison of analytical, numerical, and [9] results of $f''(0)$, $\theta'(0)$ and $\phi'(0)$ for various values of γ, with M^2=1, Re_x=1, Pr = 0.71, Sc = 0.62, Gr_x=1, Gc_x =2, n = 0.5, K=1, Sr = 0.5 and Du = 0.3.

$f''(0)$				$\theta'(0)$			$\phi'(0)$		
γ	HAM	Num	Ref [9]	HAM	Num	Ref [9]	HAM	Num	Ref [9]
0.3	-0.5192	-0.5192	-0.5716	-0.6385	-0.6318	-0.8771	-0.7117	-0.6955	-0.6794
0.5	-0.5421	-0.5420	-0.5934	-0.6154	-0.6087	-0.8960	-0.7999	-0.7755	-0.7511
0.7	-0.5618	-0.5617	-0.6133	-0.5947	-0.5879	-0.9140	-0.8798	-0.8490	-0.8181
1	-0.5867	-0.5867	-0.6399	-0.5671	-0.5603	-0.9395	-0.9879	-0.9496	-0.9113

Table 4: Comparison of analytical, numerical, and [9] results for various values of γ, with M^2=1, Re_x =1, Pr = 0.71, Sc = 0.62, Gr_x =1, Gc_x =2, n = 0.5, K=1, Sr= 0.5 and Du = 0.3.

$f''(\infty)$				$\theta'(\infty)$			$\phi'(\infty)$		
γ	HAM	Num	Ref [9]	HAM	Num	Ref [9]	HAM	Num	Ref [9]
0.3	-0.0011	-0.0011	-0.1001	-0.0012	-0.0011	-0.0459	-0.0014	-0.00144	-0.12637
0.5	-0.0010	-0.0010	-0.0950	-0.0012	-0.0012	-0.0470	-0.0012	-0.00111	-0.11337
0.7	-0.0010	-0.0009	-0.0905	-0.0013	-0.0012	-0.0480	-0.0010	-0.00102	-0.10207
1	-0.0009	0.0009	-0.0847	-0.0013	-0.0013	-0.0495	-0.0008	-0.00085	-0.08776

Table 5: Comparison of analytical, numerical, and [9] results of $f'(0)$, $\theta'(0)$ and $\phi'(0)$ for various values of M^2, with γ=1, Re_x =1, Pr = 0.71, Sc = 0.62, Gr_x =1, Gc_x =2, n = 0.5, K=1, Sr = 0.5 and Du = 0.3

$f''(0)$				$\theta'(0)$			$\phi'(0)$		
M^2	HAM	Num	Ref [9]	HAM	Num	Ref [9]	HAM	Num	Ref [9]
1	-0.5803	-0.5867	-0.6399	-0.5671	-0.5603	-0.9395	-0.9579	-0.9496	-0.9113
2	-0.9441	-0.9534	-0.9827	-0.5206	-0.5194	-0.9042	-0.9353	-0.9372	-0.8992
3	-1.2096	-1.2455	-1.2813	-0.4825	-0.4813	-0.8754	-0.9198	-0.9277	-0.8896

Table 6: Comparison of analytical, numerical, and [9] results for various values of M^2, with γ=1, Re_x =1, Pr = 0.71, Sc = 0.62, Gr_x =1, Gc_x =2, n = 0.5, K=1, Sr = 0.5 and Du = 0.3.

	$f''(\infty)$			$\theta'(\infty)$			$\phi'(\infty)$		
M^2	HAM	Num	Ref [9]	HAM	Num	Ref [9]	HAM	Num	Ref [9]
1	-0.0009	-0.0009	-0.0847	-0.0012	-0.0013	-0.0495	-0.0008	-0.0008	-0.0877
2	-0.0012	-0.0011	-0.0723	-0.0024	-0.0023	-0.0633	-0.0013	-0.0012	-0.0959
3	-0.0014	-0.0014	-0.0629	-0.0033	-0.0037	-0.0756	-0.0018	-0.0016	-0.1024

Table 7: Comparison of analytical, numerical, and [9] results of $f''(0)$, $\theta'(0)$ and $\phi'(0)$ for various values of n, with γ=1, Re_x =1, Pr = 0.71, Sc = 0.62, Gr_x =1, Gc_x =2, M^2 =1, K=1, Sr = 0.5 and Du = 0.3.

	$f''(0)$			$\theta'(0)$			$\phi'(0)$		
n	HAM	Num	Ref [9]	HAM	Num	Ref [9]	HAM	Num	Ref [9]
0.2	-0.5768	-0.5767	-0.6347	-0.4431	-0.4363	-0.8532	-.98190	-0.9766	-0.93416
0.5	-0.5852	-0.5867	-0.6399	-0.5671	-0.5603	-0.9395	-0.9379	-0.9496	-0.91135
0.9	-0.5979	-0.5964	-0.6462	-0.7160	-0.7092	-1.0469	-0.9201	-0.9164	-0.88276

Table 8: Comparison of analytical, numerical, and [9] results for various values of n, with γ=1, Re_x =1, Pr = 0.71, Sc = 0.62, Gr_x =1, Gc_x =2, M^2 =1, K=1, Sr = 0.5 and Du = 0.3.

	$f''(\infty)$			$\theta'(\infty)$			$\phi'(\infty)$		
m	HAM	Num	Ref [9]	HAM	Num	Ref [9]	HAM	Num	Ref [9]
0.2	-0.0009	-0.0009	-0.0860	-0.0014	-0.0013	-0.0563	-0.0009	-0.0008	-0.08783
0.5	-0.0008	-0.0009	-0.0847	-0.0011	-0.0013	-0.0495	-0.0008	-0.0008	-0.08776
0.9	-0.0009	-0.0008	-0.0831	-0.0010	-0.0013	-0.0415	-0.0008	-0.0008	-0.08768

Table 9: Comparison of analytical, numerical, and [9] results of $f''(0)$, $\theta'(0)$ and $\phi'(0)$ for various values of Sc, with γ=1, Re_x =1, Pr = 0.71, n = 0.5, Gr_x =1, Gc_x =2, M^2 =1, K=1, Sr = 0.5 and Du = 0.3.

	$f''(0)$			$\theta'(0)$			$\phi'(0)$		
Sc	HAM	Num	Ref [9]	HAM	Num	Ref [9]	HAM	Num	Ref [9]
0.22	-0.4711	-0.4711	-0.5572	-0.6803	-0.6735	-1.0208	-0.5707	-0.5716	-0.57932
0.42	-0.5437	-0.5402	-0.6039	-0.6159	-0.6091	-0.9754	-0.8150	-0.8015	-0.75809
0.62	-0.5897	-0.5866	-0.6399	-0.5671	-0.5603	-0.9395	-0.9779	-0.9877	-0.91135
0.82	-0.6217	-0.6220	-0.6690	-0.5261	-0.5194	-0.9098	-1.1321	-1.1511	-1.04735

Table 10: Comparison of analytical, numerical, and [9] results of $f''(\infty)$, $\theta'(\infty)$and $\phi'(\infty)$ for various values of Sc, with γ=1, Re_x =1, Pr = 0.71, n= 0.5 Gr_x =1, Gc_x =2, M^2 =1, K=1, Sr = 0.5 and Du = 0.3.

	$f''(\infty)$			$\theta'(\infty)$			$\phi'(\infty)$		
Sc	HAM	Num	Ref [9]	HAM	Num	Ref [9]	HAM	Num	Ref [9]
0.22	-0.0027	-0.0026	-0.1103	-0.0012	-0.0011	-0.0028	-0.0060	-0.0059	-0.19025
0.42	-0.0011	-0.0010	-0.0944	-0.0013	-0.0011	-0.0301	-0.0012	-0.0014	-0.12465
0.62	-0.0009	-0.0009	-0.0847	-0.0013	-0.0012	-0.0495	-0.0010	-0.0008	-0.08776
0.82	-0.0008	-0.0009	-0.0786	-0.0012	-0.0014	-0.0640	-0.0009	-0.0007	-0.06618

Table 11: Comparison of analytical, numerical, and [9] results of $f''(0)$, $\theta'(0)$and $\phi'(0)$for various values of Pr, with γ=1, Re_x =1, Sc = 0.62, n = 0.5, Gr_x =1, Gc_x =2, M^2 =1, K=1, Sr = 0.5 and Du = 0.3.

	$f''(0)$			$\theta'(0)$			$\phi'(0)$		
Pr	HAM	Num	Ref[9]	HAM	Num	Ref [9]	HAM	Num	Ref [9]
0.3	-0.5484	-0.5493	-0.6081	-0.3533	-0.3467	-0.6108	-1.0297	-1.0231	-0.9914
0.5	-0.5725	-0.5704	-0.6247	-0.4662	-0.4596	-0.7777	-1.0104	-1.0018	-0.9510
0.71	-0.5897	-0.5856	-0.6399	-0.5671	-0.5603	-0.9395	-0.9879	-0.9877	-0.9113
0.9	-0.5944	-0.5980	-0.6521	-0.6479	-0.6413	-1.0750	-0.9705	-0.9639	-0.8777

Table 12 Comparison of analytical, numerical, and [9] results of $f''(\infty)$, $\theta'(\infty)$and $\phi'(\infty)$ for various values of Pr, with γ=1, Re_x =1, Sc = 0.62, n = 0.5, Gr_x =1, Gc_x =2, M^2 =1, K=1, Sr = 0.5 and Du = 0.3.

	$f''(\infty)$			$\theta'(\infty)$			$\phi'(\infty)$		
Pr	HAM	Num	Ref [9]	HAM	Num	Ref [9]	HAM	Num	Ref [9]
0.3	-0.0040	-0.0039	-0.0993	-0.0149	-0.0144	-0.1686	-0.0020	-0.0021	-0.07475
0.5	-0.0018	-0.0017	-0.0913	-0.0038	-0.0041	-0.0996	-0.0015	-0.0013	-0.08294
0.71	-0.0008	-0.0009	-0.0847	-0.0010	-0.0013	-0.0495	-0.0011	-0.0008	-0.08776
0.9	-0.0004	-0.0006	-0.0798	-0.0004	-0.0006	-0.0178	-0.0012	-0.0006	-0.08999

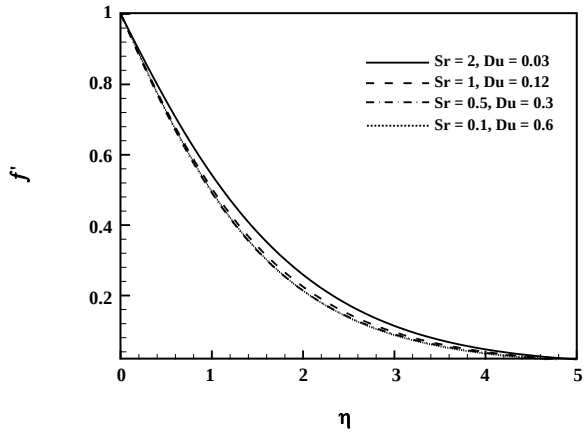

Fig. 3: Variation of velocity for different Soret and Dufour numbers (Gr=1, Gc=2, γ =1, M^2=1, Pr=0.7, n=0.5, Sc=0.62).

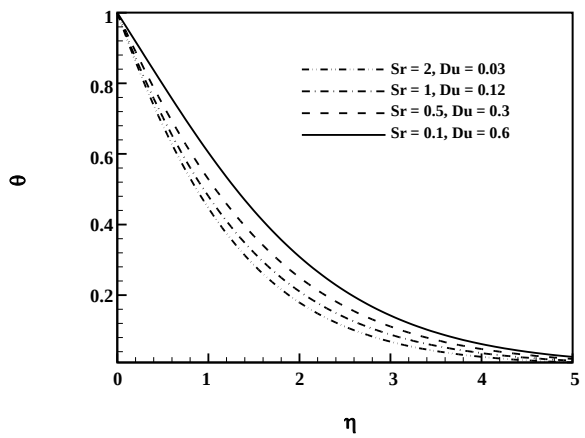

Fig. 4: Variation of temperature for different Soret and Dufour numbers (Gr=1, Gc=2, γ =1, M^2=1, Pr=0.71, n=0.5, Sc=0.62).

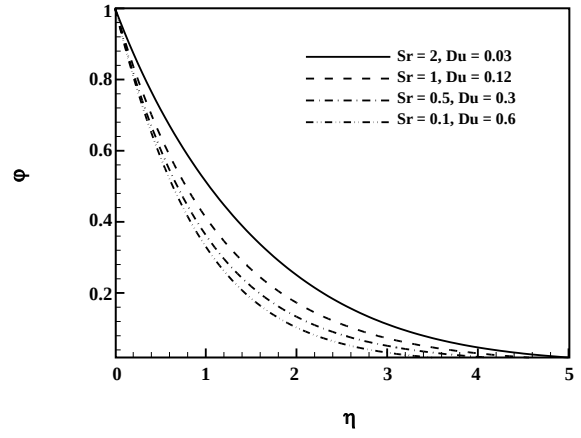

Fig. 5: Variation of concentration for different Soret and Dufour numbers (Gr=1, Gc=2, γ =1, M²=1, Pr=0.71, n=0.5, Sc=0.62).

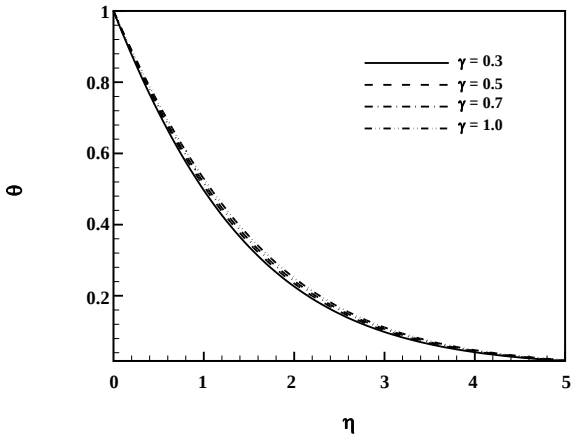

Fig. 7: Variation of temperature for different chemical reaction parameters (Gr=1, Gc=2, Du=0.3, Sr=0.5, M²=1, Pr=0.71, n=0.5, Sc=0.62).

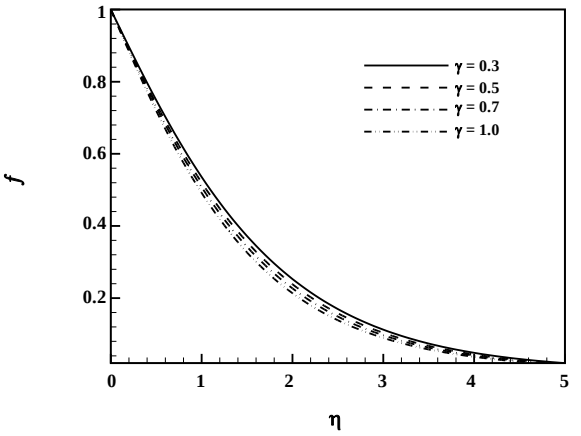

Fig. 6: Variation of velocity for different chemical reaction parameter (Gr=1, Gc=2, Du=0.3, Sr=0.5, M²=1, Pr=0.71, n=0.5, Sc=0.62).

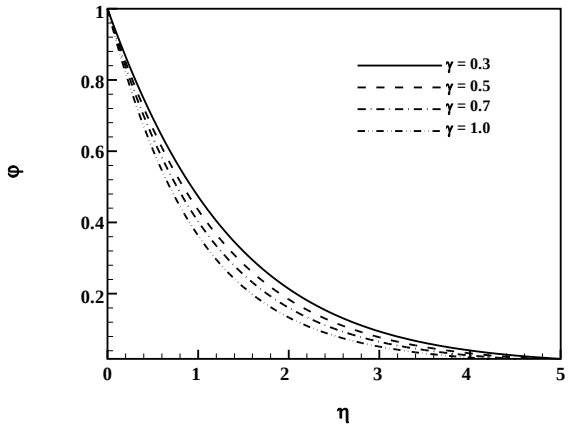

Fig. 8: Variation of concentration for different chemical reaction parameters (Gr=1, Gc=2, Du=0.3, Sr=0.5, M²=1, Pr=0.71, n=0.5, Sc=0.62).

Figs. 9–11 represent the effect of magnetic parameter on velocity, temperature and concentration respectively. It is observed that the velocity of the fluid is decreased when the magnetic parameter is increased. The values of temperature are increased when the magnetic parameter is increased, and the concentration of the fluid is increased slightly when the magnetic parameter is increased. Fig. 12 shows the effect of thermal stratification on the temperature profiles. It is observed that the temperature of the fluid is decreased when the thermal stratification parameter is increased. Fig. 13 represents the effect of Schmidt number on the velocity profiles. It is seen that the velocity of the fluid is decreased with an increase in the Schmidt number.

Fig. 14 represents the effect of Schmidt number on the temperature profiles. It is seen that the temperature of fluid is increased when the Schmidt number is increased. Fig. 15 displays the dimensionless concentration profiles for different values of Schmidt number with constant chemical reaction parameter, magnetic parameter, Soret number and Dufour number. It is understood that the concentration of the fluid is decreased when the Schmidt number is increased. Figs. 16–18 Show the effect of Prandtl number on the velocity, temperature and concentration profiles respectively. Fig. 16 shows that the velocity is decreased when the Prandtl number is increased. Fig. 17 shows that the temperature and Prandtl

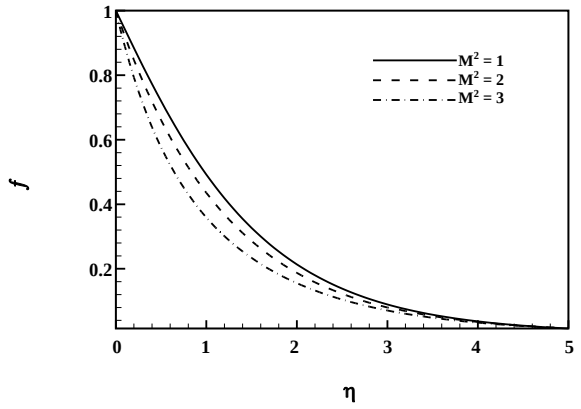

Fig. 9: Variation of velocity for different magnetic field parameters (Gr=1, Gc=2, Du=0.3, Sr=0.5, γ =1, Pr=0.71, n=0.5, Sc=0.62).

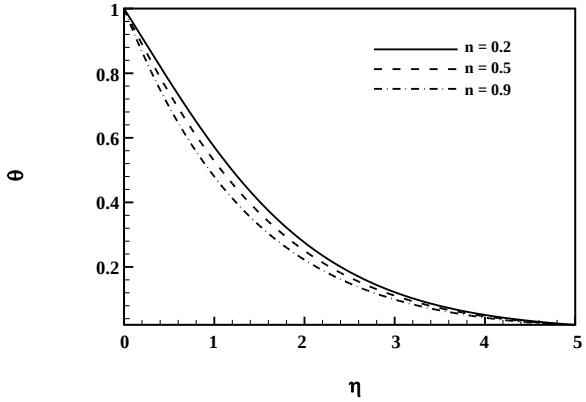

Fig. 12: Variation of temperature for different thermal stratification parameters (Gr=1, Gc=2, Du=0.3, Sr=0.5, γ=1, Pr=0.71, M^2=1, Sc=0.62).

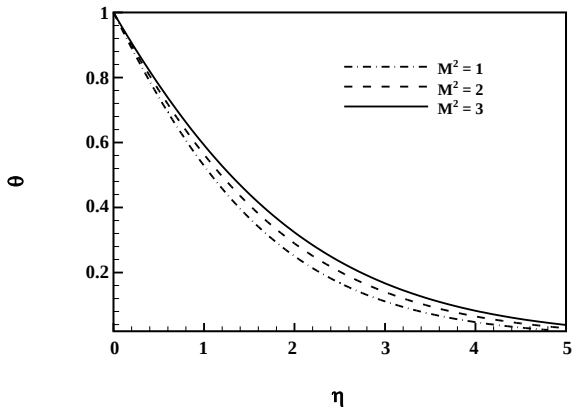

Fig. 10: Variation of temperature for different magnetic field (Gr=1, Gc=2, Du=0.3, Sr=0.5, γ=1, Pr=0.71, n=0.5, Sc=0.62).

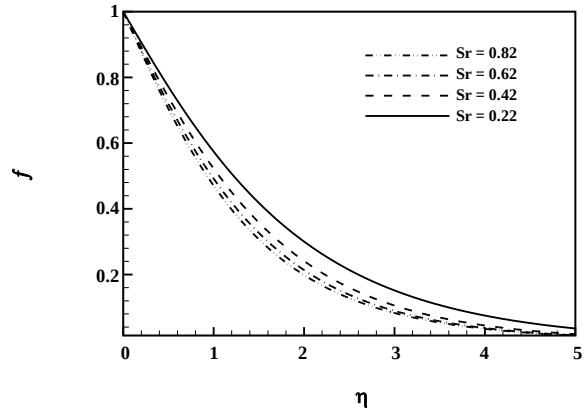

Fig. 13: Variation of velocity for different Schmidt numbers (Du=0.3, Sr=0.5, M^2=1, γ=1, Pr=0.71, n=0.5, n_1=0.5).

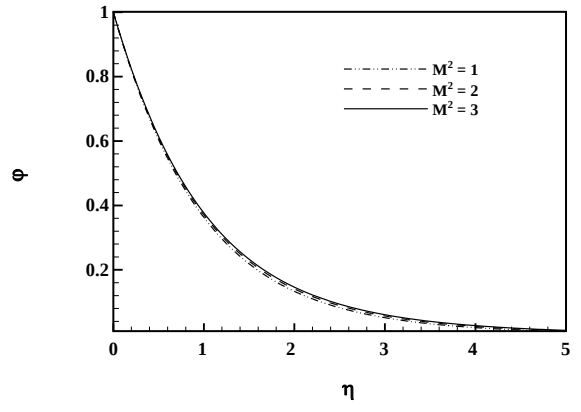

Fig. 11: Variation of concentration for different magnetic field parameters (Gr=1, Gc=2, Du=0.3, Sr=0.5, γ=1, Pr=0.71, n=0.5, Sc=0.62).

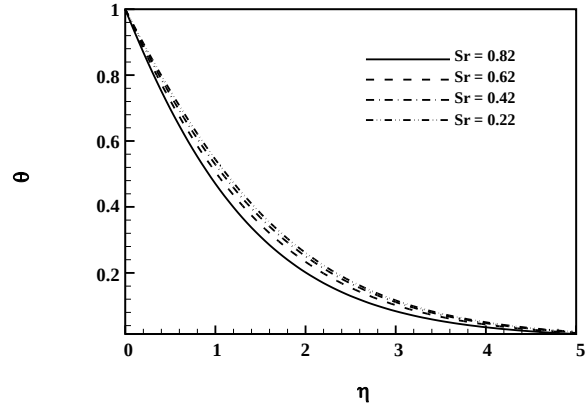

Fig. 14: Variation of temperature for different Schmidt numbers (Gr=1, Gc=2, Du=0.3, Sr=0.5, γ=1, Pr=0.71, n=0.5, M^2=1).

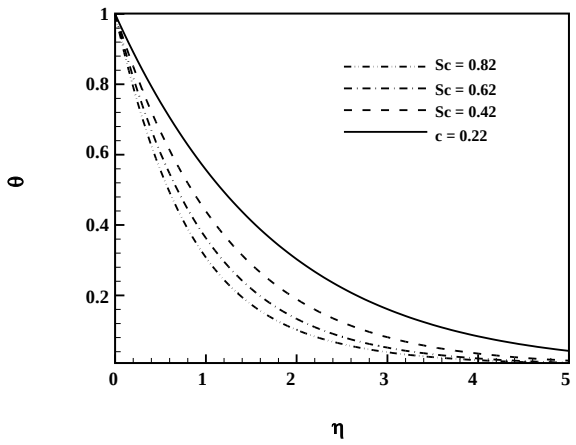

Fig. 15: Variation of concentration for different Schmidt numbers (Gr=1, Gc=2, Du=0.3, Sr=0.5, γ=1, Pr=0.71, n=0.5, M^2=1).

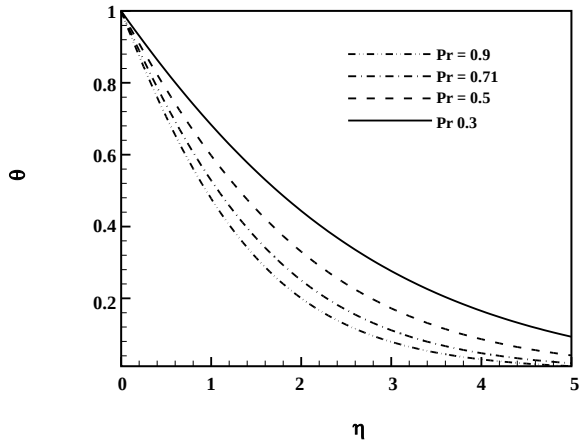

Fig. 17: Variation of temperature for different Prandtl numbers (Gr=1, Gc=2, Du=0.3, Sr=0.5, γ=1, Sc=0.62, n=0.5, M^2=1).

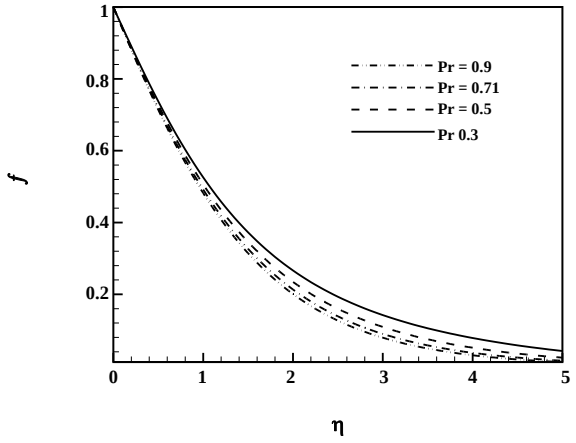

Fig. 16: Variation of velocity for different Prandtl numbers (Du=0.3, Sr=0.5, M^2=1, Sc=0.62, n=0.5, n_1=0.5, γ=1).

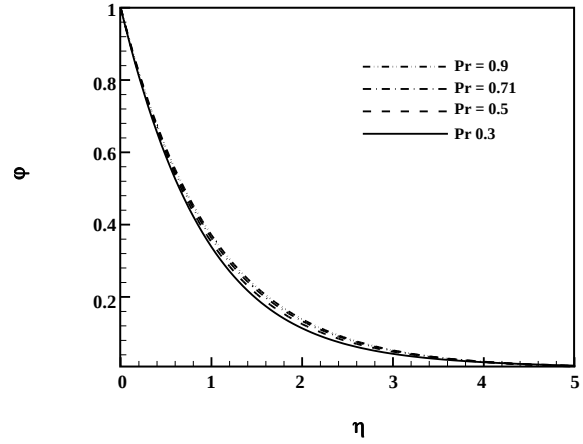

Fig. 18: Variation of concentration for different Prandtl numbers (Gr=1, Gc=2, Du=0.3, Sr=0.5, γ=1, Sc=0.62, n=0.5, M^2=1).

number are directly related to each other. It can be observed from Fig. 18 that the concentration of the fluid is increased when the Prandtl number is increased. Figs. 19-21 demonstrate the effect of Dufour number on the velocity, temperature and concentration profiles, respectively. It is understood that increasing the Dufour number causes the velocity and temperature to increase. The concentration is increased when the Dufour number is decreased.

Validation of results

The effect of Dufour number on velocity distribution is presented in Table 13. The analytical (HAM) and Ref. [9] results for velocity are compared in this table. The analytical (HAM) velocities increase when increasing Du, while the Ref. [9] velocities show a different trend. This comparison shows that either the analytical (HAM) or the Ref. [9] results must be validated. In order to verify the results, these authors had to carry out the numerical solution based on shooting method and Runge-Kutta method. The results obtained from the numerical solution are also listed in Table 13. It is noticed that the numerical results are in favor of the analytical (HAM) results, and therefore the analytical (HAM) results are substantiated.

The effect of Dufour number on concentration distribution is presented in Table 14. The analytical (HAM), numerical, and reference [9] results for

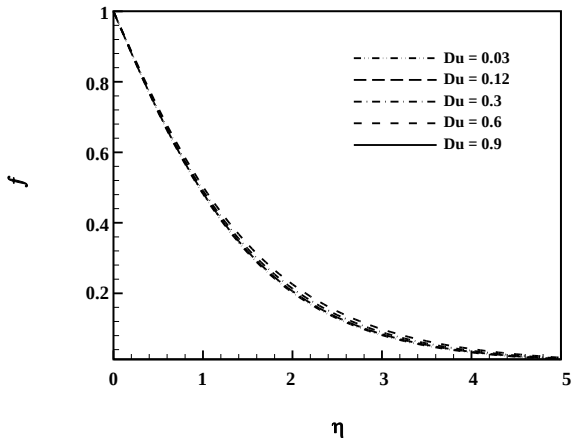

Fig. 19: Variation of velocity for different Dufour numbers (Gr=1, Gc=2, Pr=0.71, Sr=0.5, γ=1, Sc=0.62, n=0.5, M^2=1).

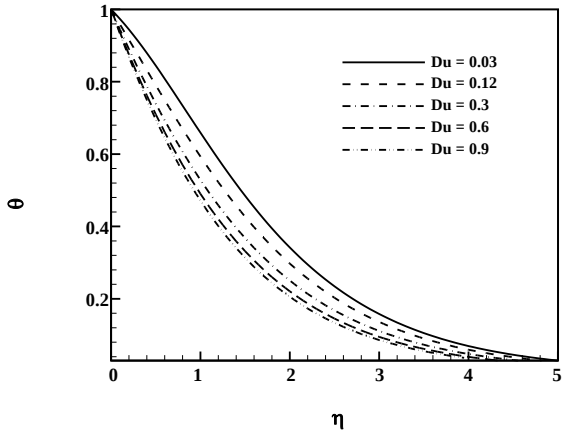

Fig. 20: Variation of temperature for different Dufour numbers (Gr=1, Gc=2, Pr=0.71, Sr=0.5, γ=1, Sc=0.62, n=0.5, M^2=1).

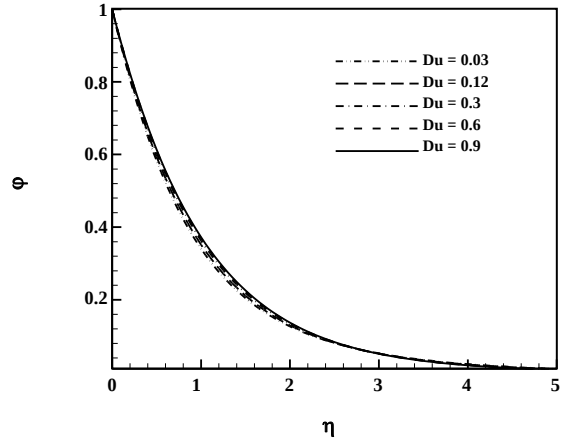

Fig. 21: Variation of concentration for different Dufour numbers (Gr=1, Gc=2, Pr=0.71, Sr=0.5, γ =1, Sc=0.62, n=0.5, M^2=1).

concentration are compared in this table. The analytical (HAM), and numerical results follow the same trend, while Ref. [9] results follow the opposite trend. This validates the analytical (HAM) results.

The effect of Dufour number on temperature distribution is presented in Table 15. The analytical (HAM), numerical, and Ref. [9] results for temperature are compared in this table. The analytical (HAM), and numerical results follow the same trend, while Ref. [9] results follow the opposite trend. This validates the analytical (HAM) results.

The effects of Dufour and Soret numbers on temperature distribution are presented in Table 16. The analytical (HAM), numerical, and Ref. [9] results for temperature are compared in this table. The analytical (HAM), and numerical results follow the same trend, while Ref. [9] results follow the opposite trend. This validates the analytical (HAM) results.

CONCLUSIONS

In this study the nonlinear differential equations resulting from similarity solution of MHD free convective heat and mass transfer of viscous, incompressible and electrically conducting fluid on a vertical stretching surface embedded in a saturated porous medium were solved using an analytical solution known as Homotopy Analysis Method (HAM) for the first time. Comparison with numerical results and the study of convergence show that using approximations of small orders, results in satisfactory accuracy and increasing the order of approximation, makes the accuracy increase. Numerical solutions for the governing equations of momentum, energy and concentration are given. Tabulated values and graphical representations are presented for the velocity, temperature and concentration for various values of Soret and Dufour numbers, chemical reaction parameter, magnetic field parameter, thermal stratification parameter, Schmidt number, and Prandtl number.

The results show that increasing the chemical reaction parameter, magnetic field strength, Schmidt number, Prandtl number and Dufour number, make the velocity of the fluid decrease. The velocity is decreased when the Soret number is decreased. The temperature is increased when the Dufour number is increased. Decreasing the Soret number, makes temperature increase,

Table 13: Comparison of analytical, numerical, and [9] results of f' for various values of Du, with γ=1, Re_x =1, Sc=0.62, n = 0.5, Gr_x =1, Gc_x =2, M^2 =1, K=1, Sr = 0.5.

Du	*f*' (1)	Num	Ref [9]
0.03	0.4817	0.4817	0.4547
0.12	0.485	0.485	0.4455
0.3	0.4917	0.4917	0.4302
0.6	0.5027	0.5027	0.4200
0.9	0.5136	0.5136	0.4149
Du	*f*' (2)	Num	Ref [9]
0.03	0.2021	0.2021	0.1478
0.12	0.206	0.206	0.1386
0.3	0.2136	0.2136	0.1325
0.6	0.2257	0.2257	0.1263
0.9	0.2371	0.2371	0.1203
Du	*f*' (3)	Num	Ref [9]
0.03	0.0811	0.0812	-
0.12	0.084	0.0839	-
0.3	0.0896	0.0895	-
0.6	0.0981	0.0985	-
0.9	0.1057	0.1057	-
Du	*f*' (4)	Num	Ref [9]
0.03	0.0321	0.032	-
0.12	0.0338	0.0385	-
0.3	0.0371	0.037	-
0.6	0.0419	0.042	-
0.9	0.0461	0.0462	-
Du	*f*' (5)	Num	Ref [9]
0.03	0.0124	0.0124	-
0.12	0.0133	0.0136	-
0.3	0.015	0.0148	-
0.6	0.0174	0.0167	-
0.9	0.0194	0.0193	-

Table 14: Comparison of analytical, numerical, and [9] results of ϕ for various values of Du, with γ=1, Re_x =1, Sc =0.62, n = 0.5, Gr_x =1, Gc_x =2, M^2 =1, K=1, Sr = 0.5.

Du	ϕ (1)	Num	Ref [9]
0.03	0.3726	0.3726	0.3634
0.12	0.3694	0.3694	0.3779
0.3	0.3628	0.3628	0.3887
0.6	0.3517	0.3517	0.3995
0.9	0.3405	0.3405	0.4212
Du	ϕ (2)	Num	Ref [9]
0.03	0.1372	0.1372	0.1023
0.12	0.1358	0.1358	0.1167
0.3	0.1333	0.1333	0.1239
0.6	0.1297	0.1297	1.2600
0.9	0.1267	0.1267	0.1312
Du	ϕ (3)	Num	Ref [9]
0.03	0.0514	0.0513	-
0.12	0.0514	0.0512	-
0.3	0.0515	0.0516	-
0.6	0.0519	0.052	-
0.9	0.0525	0.0524	-
Du	ϕ (4)	Num	Ref [9]
0.03	0.0197	0.0195	-
0.12	0.02	0.021	-
0.3	0.0207	0.0205	-
0.6	0.0217	0.0216	-
0.9	0.0228	0.0225	-
Du	ϕ (5)	Num	Ref [9]
0.03	0.0076	0.0077	-
0.12	0.0079	0.0079	-
0.3	0.0084	0.0084	-
0.6	0.0092	0.0092	-
0.9	0.0099	0.0099	-

Table 15: Comparison of analytical, numerical, and [9] Results of θ for various values of Du, with γ=1, Re_x =1, Sc = 0.62, n = 0.5, Gr_x =1, Gc_x =2, M^2 =1, K=1, Sr = 0.5.

Du	θ (1)	Num	Ref [9]
0.03	0.4713	0.4713	0.4206
0.12	0.4902	0.4902	0.3922
0.3	0.5284	0.5284	0.3418
0.6	0.5931	0.5931	0.2597
0.9	0.6592	0.6592	0.1777
Du	θ (2)	Num	Ref [9]
0.03	0.2054	0.2054	0.1377
0.12	0.2206	0.2206	0.1188
0.3	0.2503	0.2503	0.0904
0.6	0.2974	0.2974	0.0400
0.9	0.3417	0.3417	0.0000
Du	θ (3)	Num	Ref [9]
0.03	0.0861	0.086	-
0.12	0.0947	0.0946	-
0.3	0.1111	0.1111	-
0.6	0.136	0.136	-
0.9	0.158	0.158	-
Du	θ (4)	Num	Ref [9]
0.03	0.0352	0.0351	-
0.12	0.0394	0.0393	-
0.3	0.0474	0.0475	-
0.6	0.0591	0.0593	-
0.9	0.0693	0.0689	-
Du	θ (5)	Num	Ref [9]
0.03	0.0139	0.0139	-
0.12	0.0158	0.0158	-
0.3	0.0194	0.0194	-
0.6	0.0246	0.0245	-
0.9	0.0291	0.0292	-

Table 16: Comparison of analytical, numerical, and [9] Results of θ for various values of Du and Sr, with γ=1, Re_x =1, Sc = 0.62, n = 0.5, Gr_x =1, Gc_x =2, M^2 =1, K=1.

Du	Sr	θ (1)	Num	Ref [9]
0.03	2	0.4469	0.4469	0.4103
0.1	1	0.4803	0.4802	0.3883
0.3	0.5	0.5284	0.5284	0.3370
0.6	0.1	0.6043	0.6043	0.2491
Du	Sr	θ (2)	Num	Ref [9]
0.03	2	0.179	0.179	0.1209
0.1	1	0.2106	0.2106	0.1062
0.3	0.5	0.2503	0.2503	0.0806
0.6	0.1	0.3091	0.3091	0.0330
Du	Sr	θ (3)	Num	Ref [9]
0.03	2	0.0681	0.068	-
0.1	1	0.0882	0.0883	-
0.3	0.5	0.1111	0.113	-
0.6	0.1	0.1424	0.145	-
Du	Sr	θ (4)	Num	Ref [9]
0.03	2	0.0252	0.0253	-
0.1	1	0.0359	0.0359	-
0.3	0.5	0.0474	0.0475	-
0.6	0.1	0.0615	0.0613	-
Du	Sr	θ (5)	Num	Ref [9]
0.03	2	0.0091	0.0092	-
0.1	1	0.0142	0.0141	-
0.3	0.5	0.0194	0.0195	-
0.6	0.1	0.0251	0.0253	-

the temperature is decreased when the thermal stratification parameter, or Prandtl number are increased. Temperature is decreased slightly when the chemical reaction parameter is increased. The temperature is increased when the magnetic field parameter or Schmidt number is increased. The concentration is decreased when the Soret number is increased, or the Dufour number is decreased, or the chemical reaction and Schmidt number are increased. Concentration is slightly increased when the magnetic field is increased.

Nomenclature

B_0	Magnetic field strength
C	Concentration
C_p	Specific heat at constant pressure
C_s	Concentration susceptibility
D_m	Mass diffusivity
Du	Dufour numbe
f'	Dimensionless velocity
G	Gravitational acceleration
Gr	Grash of number

Gc	Modified Grashof number
H(η)	Auxiliary function
HAM	Homotopy analysis method
h	Auxiliary parameter
k	Thermal conductivity
K	*Darcy* permeability
K_1	Permeability of porous medium
K_T	Thermal diffusion ratio
K_c	Rate of chemical reaction
m	Order of deformation equation
M^2	Magnetic parameter
MHD	Magneto hydrodynamic
n	Thermal stratification parameter
n_1	Concentration stratification parameter
Pr	Prandtl number
q	Embedding parameter
Re	Reynolds number
Sc	Schmidt number
Sr	Soret number
T	Temperature
U_0	Velocity
β	Coefficient of volumetric expansion
η	Dimensionless coordinate
γ	Chemical reaction parameter
σ	Electrical conductivity
ρ	Density of the fluid
ν	Kinematic viscosity
θ	Dimensionless temperature
ϕ	Dimensionless concentration

Subscripts

C	Concentration
m	Mean
T	Temperature
w	Wall
x	Local
∞	Infinity

Received : Sept. 16, 2014 ; Accepted : Dec. 21, 2015

REFERENCES

[1] Kandasamy R., Periasamy K., Nonlinear Hydro Magnetic Flow, Heat and Mass Transfer Over an Accelerating Vertical Surface with Internal Heat Generation and Thermal Stratification Effects, *Journal of Computational and Applied Mechanics*, **6**(1): 27-37 (2005).

[2] Shariful Alam Md., Rahman M.M., Abdul Maleque Md., Local Similarity Solutions for Unsteady MHD Free Convection and Mass Transfer Flow Past an Impulsively Started Vertical Porous Plate with Dufour and Soret Effects, *Thammasat International Journal of Science and Technology*, **10**(3): 1-8 (2005).

[3] Shariful Alam Md., Rahman M.M., Samad M.A., Dufour and Soret Effects on Unsteady MHD Free Convection and Mass Transfer Flow Past a Vertical Porous Plate in a Porous Medium, *Nonlinear Analysis: Modelling and Control*, **11**(3): 217–226 (2006).

[4] Raptis A., Kafoussias N.G., Magneto Hydrodynamic Free Convection Flow and Mass Transfer Through Porous Medium Bounded by an Infinite Vertical Porous Plate with Constant Heat Flux, *Canadian Journal of Physics*, **60**(12): 1725–1729 (1982).

[5] Anghel M., Takhar H.S., Pop I., Soret and Dufour Effects on Free-Convection Boundary Layer Over a Vertical Surface Embedded in a Porous Medium, *Studia Universitatis Babes-Bolyai, Mathematica*, **45**(4): 11–21 (2000).

[6] Postelnicu A., Influence of a Magnetic Field on Heat and Mass Transfer by Natural Convection from Vertical Surfaces in Porous Media Considering Dufour and Soret Effects, *International Journal of Heat and Mass Transfer*, **47**(6–7): 1467–1472 (2004).

[7] Shariful Alam Md., Rahman M.M., Dufour and Soret Effects on MHD Free Convective Heat and Mass Transfer Flow Past a Vertical Flat Plate Embedded in a Porous Medium, *Journal of Naval Architecture and Marine Engineering.*, **2**(1): 55-65 (2005).

[8] El-Kabeir S.M.M., Modather M., Abdou M., Chemical Reaction, Heat and Mass Transferon MHD Flow Over a Vertical Isothermal Cone Surface in Micro-Polar Fluids with Heat Generation/ Absorption, *Applied Mathematical Sciences*, **1**(34): 1663-1674 (2007).

[9] Mansour M.A., El-Anssary N.F., Aly A.M., Effects of Chemical Reaction and Thermal Stratification on MHD Free Convective Heat and Mass Transfer Over a Vertical Stretching Surface Embedded in a Porous Media Considering Soret and Dufour Numbers, *Chemical Engineering Journal*, **145**: 340-345 (2008).

[10] Liao S.J., "The Proposed Homotopy Analysis Technique for the Solution of Nonlinear Problems", Ph.D. Thesis, Shanghai Jiao Tong University, (1992).

[11] Kimiaeifar A., "Application of HAM, PEM and HPM to Find Analytical Solution for Nonlinear Problems in Solid Mechanics", M.Sc. Thesis, Shahid Bahonar University of Kerman, (2008).

[12] Sajid M., Hayat T., Comparison of HAM and HPM Methods in Nonlinear Heat Conduction and Convection Equations, *Nonlinear Analysis: Real World Applications*, **9**(5): 2296-2301 (2008).
(doi:10.1016/j.nonrwa.2007.08.007)

[13] Chowdhury M.S.H., Hashim I., Abdulaziz O., Comparison of Homotopy Analysis Method and Homotopy-Perturbation Method for Purely Nonlinear Fin-Type Problems, *Communications in Nonlinear Science and Numerical Simulation*, **14**(2): pp. 371-378 (2009).
(doi:10.1016/j.cnsns.2007.09.005)

[14] Rahimpour M., Mohebpour S.R., Kimiaeifar A., Bagheri G.H., On the Analytical Solution of Axisymmetric Stagnation Flow Towards a Shrinking Sheet, *International Journal of Mechanics*, **2**: 1–10 (2008).

[15] Kimiaeifar A., Saidi A.R., Analytical Solution for Stress Analysis in Hollow Cylinder Made of Functionally Graded Materials, "Proceedings of the 16th International Conference on Mechanical Engineering, Kerman, Iran", 13-15 May (2008) *(ISME2008)*.

[16] Domairry G., Mohsenzadeh A., Famouri M., The Application of Homotopy Analysis Method to Solve Nonlinear Differential Equation Governing Jeffery–Hamel Flow, *Communications in Nonlinear Science*, **14**: 85-95 (2009).

[17] Hayat T., Khan S.B., Khan M., Exact Solution for Rotating Flows of a Generalized Burgers' Fluid in a Porous Space, *Applied Mathematical Modelling*, **32**: 749-760 (2008).

[18] Kimiaeifar A., Saidi A.R., Bagheri G.H., Rahimpour M., Analytical Solution for Van Der Pol –Duffing Oscillators, *Chaos, Solitons and Fractals*, **42**(5): 2660-2666 (2009).

[19] Fooladi M., Abaspour S.R., Kimiaeifar A., Rahimpour M., On the Analytical Solution of Nonlinear Normal Mode for Continuous Systems by Means of HAM, *World Applied Sciences Journal*, **6**(3): 297-302 (2009).

[20] Kimiaeifar A., Bagheri G.H., Rahimpour M., Mehrabian M.A., Analytical Solution of Two-Dimensional stagnation Flow in the Vicinity of a Shrinking Sheet by Means of Homotopy Analysis Method, *Journal of Process Mechanical Engineering*, Institution of Mechanical Engineers, Part E, **223**(3): 133-143 (2009.